ENGINEERING TRANSACTIONS • *Engng. Trans.* • **64**, 4, 547–553, 2016
Polish Academy of Sciences • Institute of Fundamental Technological Research (IPPT PAN)
National Engineering School of Metz (ENIM) • Poznan University of Technology

A Numerical Investigation of the Influence of the Material Microstructure on the Failure Mode of Metal Ceramic Composites

Pitchai PANDI, Gabriella BOLZON

Department of Civil and Environmental Engineering
Politecnico di Milano
Piazza Leonardo da Vinci 32, 20133 Milano, Italy
e-mail: gabriella.bolzon@polimi.it

Metal failure is often initiated by strain localization in narrow bands. In metal matrix composites, the occurrence and the consequences of this phenomenon are influenced by the material microstructure. This dependency has been numerically investigated by considering periodic and quasi-periodic arrangement of ceramic fibers in a metal matrix, with reinforcement content varying between 10% and 50% in volume. The constitutive response of the metal has been simulated by the widely used GTN (Gurson-Tvergaard-Needleman) continuum damage-plasticity model with evolution law based on local porosity. The onset of failure for the composite has been identified with the critical growth of micro voids that induce softening at the macro scale. An extensive study has been performed in order to distinguish the effects of the material microstructure, the role of the imperfections and the influence of the simulation details. The main results of this investigation are summarized in this paper.

Key words: metal ceramic composites, numerical simulation, failure analysis.

1. Introduction

Metal ceramic composites are exploited in several industrial sectors (e.g., aerospace, automotive, biomedical, energy) for the peculiar characteristics induced by this coupling: high specific strength and stiffness; lightweight; good wear, thermal, corrosion and fracture resistance [1–5]. The overall characteristics of these material systems depend on several micromechanical features, and can be strongly influenced by local imperfections. Significant consequences may for instance arise from the residual porosity left in the metal matrix by the composite fabrication process [6].

The macroscopic damage resulting from the growth and coalescence of micro voids under external actions can be estimated by means of numerical simulations based on the so-called GTN constitutive law introduced by GURSON [7] and improved by TVERGAARD [8] and NEEDLEMAN [9]. This failure model has been experimentally validated for several ductile metals exploited in demanding industrial contexts [10, 11]. The main results of an investigation concerning fiber reinforced metal matrix composites are summarized in this contribution.

2. Model problem

Regular and quasi-regular packing of cylindrical ceramic fibers embedded in a metal matrix has been considered, varying the reinforcement content between 10% and 50% in volume. The overall response of the resulting composites has been recovered by numerical homogenization on the representative volume elements (RVEs) shown for instance in Fig. 1. Uniaxial (on the macroscopic scale) material extension in the direction transversal to the fiber axis has been simulated in plane strain conditions. Computations have been carried out by a popular finite element code [12], accounting for both material and geometric non-linearity. Different discretized models of the problem domains have been taken into account, implementing regular (radial-circumferential) and random mesh subdivision. Periodic displacement distribution [13] has been enforced by means of linear constraint equations linking the degrees of freedom on the boundary of the RVE.

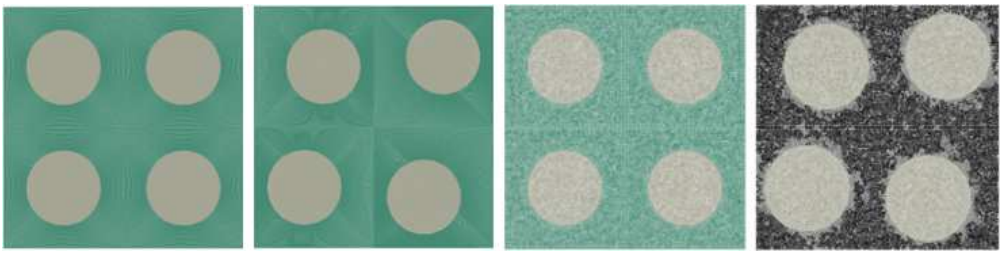

FIG. 1. The assumed RVEs and the domain discretization for 40% ceramic volume content.

The effective material response has been evaluated for different volume ratio of the constituents, here supposed to be aluminum (Al) and silicon carbide (SiC). Linear elastic constitutive law, isotropic in the considered plane, has been assumed for SiC, characterized by the elastic modulus 420 GPa and by 0.25 lateral contraction coefficient. The metal response to external actions has been described instead by the phenomenological GTN damage-plasticity model.

In GTN formulation, the yield function Φ is defined as:

$$\Phi = \left(\frac{q}{\sigma_y}\right)^2 + 2q_1 f^* \cosh\left(-q_2 \frac{3p}{2\sigma_y}\right) - \left(1 + q_3 f^{*2}\right), \tag{2.1}$$

where p and q represent the mean stress and the equivalent deviatoric (Mises) stress, respectively, while f^* indicates the effective porosity. This latter quantity is associated to the volume fraction f of the micro voids in the metal by the relationships:

$$f^* = \begin{cases} f & f \leqslant f_c, \\ f_c + \dfrac{f_u - f_c}{f_f - f_c}(f - f_c) & f_c \leqslant f < f_f, \\ f_u = \dfrac{q_1 + \sqrt{q_1^2 - q_3}}{q_3} & f \geqslant f_f. \end{cases} \tag{2.2}$$

Plastic strains control the evolution (growth and nucleation) of the void content according to the rate expression:

$$\dot{f} = (1 - f)\dot{v}^p + \left(\frac{f_N}{S_N\sqrt{2\pi}} \exp\left[-\frac{1}{2}\left(\frac{e^p - \varepsilon_N}{S_N}\right)^2\right]\right)\dot{e}^p, \tag{2.3}$$

where v^p and e^p represent, respectively, the plastic amount of the volumetric strain and of the equivalent strain conjugate to q. The cumulated equivalent plastic strain e^p governs also the hardening behavior of the metal through the exponential rule:

$$\sigma_y = \sigma_{y0}\left(1 + \frac{Ee^p}{\sigma_{y0}}\right)^n. \tag{2.4}$$

Several symbols introduced with relations (2.1)–(2.4) represent model parameters. In particular: the elastic modulus $E = 72.4$ GPa and the lateral contraction coefficient (here assumed equal to 0.33) describe the elastic response of the metal matrix within the domain defined by the initial yield stress $\sigma_{y0} = 240$ MPa and by the hardening exponent $n = 0.1$; the critical and final porosity values (f_c and f_f, respectively) limit the void coalescence range; f_N modulates the nucleation rate of new voids; ε_N and S_N represent, respectively, the mean value and the standard deviation of the statistical (Gaussian) distribution of residual strains resulting from the production process. The value f_u represents the upper bound for the effective porosity f^*, in correspondence of which the stress carrying capacity of the material is annihilated; f_u depends on parameters q_1, q_2 and q_3 as shown by (2.2), derived from the condition $\Phi = 0$

when stress invariants p and q are null. The assumed values of the nine material constants related to porosity in GTN model reported in Table 1, have been selected from literature data (e.g., [9–11] and references therein). The initial volume fraction of voids in the metal matrix, f_0, is also indicated.

Table 1. Assumed values of the constitutive parameters governing the evolution of micro voids.

q_1	q_2	q_3	f_0	f_c	f_f	f_N	ε_N	S_N
1.5	1.0	2.25	0.01	0.1	0.2	0.04	0.3	0.1

3. Selected results

The graphs drawn in Fig. 2 represent the effective response of the considered composite materials, recovered by numerical homogenization for 10% and 40% ceramic content. The curves visualize the relationship between the macroscopic stress and the corresponding strain in the stretched direction. The graphs evidence that the overall material strength is not affected by the volume fraction of the reinforcement, while ductility is significantly reduced for higher ceramic content. The post-peak decay is influenced either by the regularity of the fiber distribution and by the finite element discretization, with anticipated softening threshold in the more realistic hypothesis of uneven microstructure.

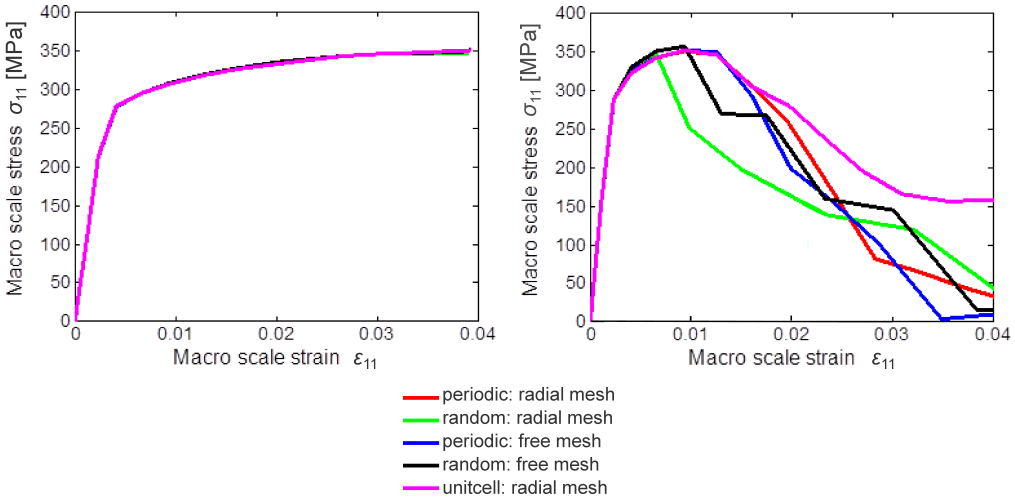

Fig. 2. Macroscopic response of the investigated composites with 10% (left) and 40% (right) ceramic content.

The observed features of the macroscopic material response reflect local details. In particular, strains are intensified in correspondence of the fibers, which promote the formation of localization bands in the metal matrix.

The distribution of the plastic strains cumulated in the matrix at the onset of softening is visualized in Fig. 3 and Fig. 4. In the case of periodic fiber arrays, strain localization lines are straight and develop: almost freely in the metal for low ceramic content; along preferential directions for larger diameters. Uneven reinforcement distribution enhances the inelastic effects, further emphasized in the case of high ceramic content. In the most severe conditions, high plastic

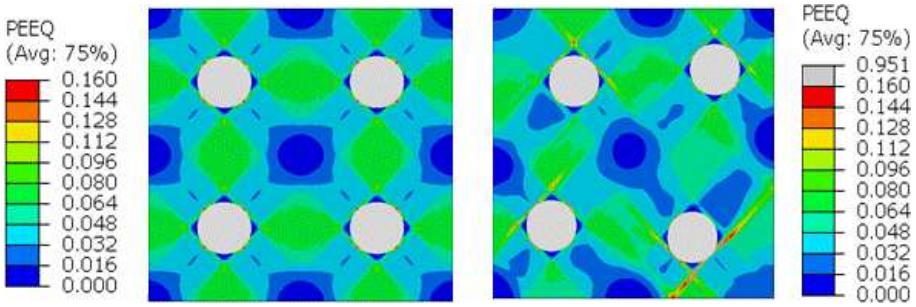

FIG. 3. Plastic strain distribution in the metal matrix for 10% ceramic content at 3.9% macroscopic strain: regular fiber arrangement on the left, uneven on the right.

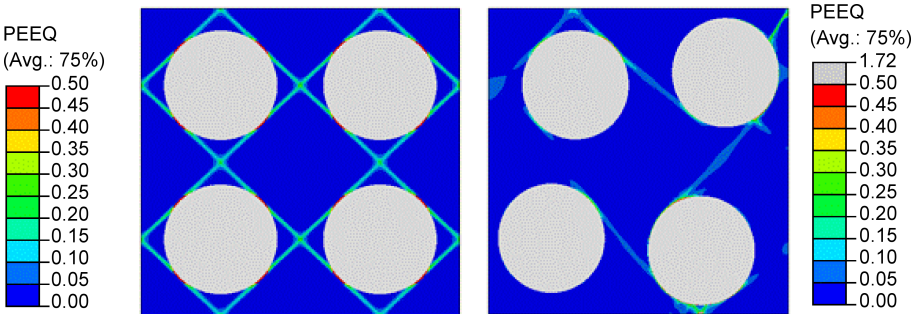

FIG. 4. Plastic strain distribution in the metal matrix for 40% ceramic content at 1.6% macroscopic strain: regular fiber arrangement on the left, uneven on the right.

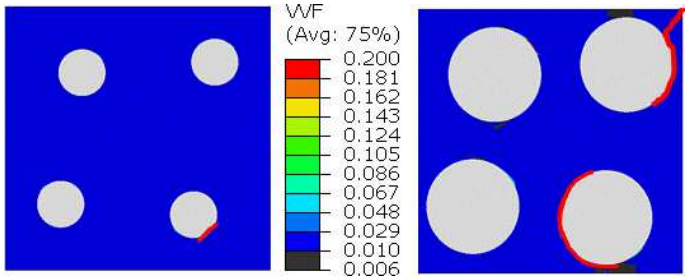

FIG. 5. Void volume fraction distribution in the metal matrix for uneven fiber arrangement: 10% ceramic content at 3.9% macroscopic strain on the left; 40% ceramic content at 1.6% macroscopic strain on the right.

strain lines break into segments of varying direction, provoke the growth and nucleation of voids around the interface with the inclusions as shown in Fig. 5, and promote debonding.

4. Closing remarks

The connection between microstructural details and the overall response of metal matrix composites has been numerically investigated, considering ideal regular arrays of embedded elastic ceramic fibers and a more realistic uneven distribution of the reinforcement. The presence and the evolution under external actions of micro voids in the matrix has been described by a widely used continuum damage-plasticity model characterized by the contribution of the local porosity. The simulations evidence an apparent reduction of the material ductility with the increase of the volume fraction of the reinforcement. Concentration of micro voids at the interface with the fibers, inducing possible debonding phenomena, has been also detected for high ceramic content.

References

1. Kaczmar J.W., Pietrzak K., Włosiński W., *The production and application of metal matrix composite materials,* Journal of Materials Processing Technology, **106**(1–3): 58–67, 2000, doi: 10.1016/S0924-0136(00)00639-7.
2. Evans A., San Marchi C., Mortensen A., *Metal matrix composites in industry: an introduction and a survey*, Springer Science, New York, 2003.
3. Fan S., Zhang L., Xu Y., Cheng L., Tian G., Ke S., Xu F., Liu H., *Microstructure and tribological properties of advanced carbon/silicon carbide aircraft brake materials*, Composites Science and Technology, **68**(14): 3002–3009, 2008, doi: 10.1016/j.compscitech.2008.06.013.
4. Qu X.-H., Zhang L., Wu M., Ren S.-B., *Review of metal matrix composites with high thermal conductivity for thermal management application*, Progress in Natural Science: Materials International, **21**(3): 189–197, 2011, doi: 10.1016/S1002-0071(12)60029-X.
5. Macke A.J., Schultz B.F., Rohatgi P.K., *Metal matrix composites offer the automotive industry an opportunity to reduce vehicle weight, improve performance*, Advanced Materials & Processes, **170**(3): 19–23, 2012.
6. Babout L., Maire E., Buffičre J.Y., Fougčres R., *Characterization by X-ray computed tomography of decohesion, porosity growth and coalescence in model metal matrix composites*, Acta Materialia, **49**(11): 2055–2063, 2001, doi: 10.1016/S1359-6454(01)00104-5.
7. Gurson A.L., *Continuum theory of ductile rupture by void nucleation and growth: Part I – Yield criteria and flow rules for porous ductile media*, ASME Journal of Engineering Materials and Technology, **99**(1): 2–15, 1977, doi: 10.1115/1.3443401.
8. Tvergaard V., *On localization in ductile materials containing spherical voids*, International Journal of Fracture, **18**(4): 237–252, 1982, doi: 10.1007/BF00015686.

9. Needleman A., Tvergaard V., *Analysis of ductile rupture in notched bars*, Journal of the Mechanics and Physics of Solids, **32**(6): 461–490, 1984, doi: 10.1016/0022-5096(84)90031-0.

10. Lievers W.B., Pilkey A.K., Lloyd D.J., *Using incremental forming to calibrate a void nucleation model for automotive aluminum sheet alloys*, Acta Materialia, **52**(10): 3001–3007, 2004, doi: 10.1016/j.actamat.2004.03.002.

11. He M., Li F., Wang Z., *Forming limit stress diagram prediction of aluminum alloy 5052 based on GTN model parameters determined by in situ tensile test*, Chinese Journal of Aeronautics, **24**(3): 378–386, 2011, doi: 0.1016/S1000-9361(11)60045-9.

12. Abaqus/Explicit, release 6.13-1, Dassault Systems Simulia Corp, Providence, RI, USA, 2013.

13. Michel J.C., Moulinec H., Suquet P., *Effective properties of composite materials with periodic microstructure: a computational approach*, Computer Methods in Applied Mechanics and Engineering, **172**: 109–143, 1999.

Received October 14, 2016; accepted version November 9, 2016.